Basrah Journal for Engineering Sciences, Vol. 20, No. 2, (2020), 27-33

Basrah Journal for Engineering Sciences

Journal homepage: www.bjes.edu.iq
ISSN (Online): 23118385, ISSN (Print): 18146120

OPEN ACCESS

Estimation of Submerged Arc Plates Weldment Properties Using ANFIS and Regression Techniques

Abdul Kareem F. Hassan [1,*], Raad Jamal Jasim [2], Yousif Younis Ashoor [3]

[1,2,3]*Department of Mechanical Engineering, College of Engineering, University of Basrah, Basrah, Iraq*
E-mail addresses: abdulkareem.flaih@uobasrah.edu.iq , Raad.jassim@uobasrah.edu.iq
Received: 13 February 2019; Accepted: 23 December 2019; Published: 2 March 2020

Abstract

The present work aims to build mathematical models based on experimental data to estimate the mechanical properties of submerged arc weldment. AISI 1020 low carbon steel plates 16mm thickness were welded according to orthogonal array in order to establish the relationship between input parameters (welding current, Arc voltage and welding speed) and output parameters (ultimate tensile stress, yield stress, impact energy and hardness) by submerged arc welding (SAW) process. The relationship between input and output parameters for the welding process are conducted using two suitable mathematical models the first one based on regression analysis, while the second one based on multi input single output ANFIS model for estimation of some mechanical properties of the welded plates. It was found that ANFIS results are closer to the experimental results than regression results. The optimal parameters (which give a maximum value of ultimate tensile strength (UTS), yield stress and impact energy; 446 MPa, 318 MPa and 213 J) are welding current is (380 Amp), Arc voltage is (25 V) and welding speed is (40 cm/min), while the maximum value of hardness number is (228 HV), when current welding is (380 Amp), Arc voltage is (25 V) and welding speed is (25 cm/min).

Keywords: ANFIS, Regression analysis.

1. Introduction

The American Welding Society (AWS) defined welding as a localization coalescence (the fusion or growing to gather of the grain structure of the materials being welded) of metallic or non-metallic material that produced by heating the material to the required welding temperature, with or without the application of pressure, or by the application of pressure alone with or without using of filler materials. There are two major classify of the welding process and also, defined by American Welding Society (AWS). There are two major classify of the welding process [1]:

(i) Solid state welding: produce coalescence by welding process by application of pressure at a temperature lower than the temperature of the base.

(ii) Fusion welding: any welding process produces by fusion of the base metal in order to make the weld. Lee and Um in (2000) [2], employed ANN and analysis for multiple regression to the geometry forecast of back-bead in (GMAW). The current of welding, gap, arc voltage and speed of welding were the independent parameters can be used in the analysis of multiple regression and the dependent parameters such as depth and width of the back-bead. The method of ANN showed superior results to the analysis of multiple regressions in the field rate of error prediction. It is noticed that the rate of error predicted the width was less accurate than the depth of the back-bead. In addition, the analysis results show prediction regression of equation for the welding process parameters were modeled to obtain the desired the bead of geometry by performing inverse transformation for the model of the multiple regressions of width and of back-bead have a maximum error of prediction below then 6.5 %. Juang and Tarng in (2002) [3], modified Taguchi method to analyze the effect of tungsten inert gas (TIG) and depending on bead geometry for the weld pool that has four smaller-the-better characteristics quality (i) front width, (ii) back width, (iii) front height, and (iv) back height, and also to determine optimal parameters for bead geometry of the weld. TIG experiments are carried out with an arc gap the range of 1.7-2.6 mm, the welding current in the range of 40-55 A, the flow rate in the range 8-11 l/mm and the welding speed in the range of 13.5-15 cm/min. The experimental results showed that using the Taguchi approach improves the weld pool in the TIG welding of stainless steel. Hancheng et al. in (2002) [4], used the experimental data for material properties to model extracted fuzzy rules by using (ANFIS) to estimate the tensile strength depends on the microstructure and compositions. To verify the model 38 experiments were done, divided into 29 cases for the training and 9 cases for the testing .The membership functions of the input were chosen as Gaussian type. The input for (ANFIS) was (carbon equivalent, micro hardness of the matrix, the graphite flake size, the amount eutectic cell and the amount austenite dendrite. Kim et al. in (2003) [5], explained the relationship among process variables like arc voltage, current, welding angle, welding speed on bead penetration of plate welds. They developed linear and curvilinear mathematical models and controlling the automated/robotic CO_2 arc welding process to select the best model. According to the experimental results they founds that welding speed is the most variant that affect the penetration of the bead in the CO_2 arc welding process. Kumanan et al. in (2007) [6], presented regression analysis and determine the optimal parameters with the application of Taguchi technique using

semiautomatic (SAW) process. They construct the relationships between the dependent and independent variables: reinforcement of the weld, the depth of penetration, bead width and hardness with arc voltage, current, electrode stick out and welding speed. Multiple regression analysis was conducted using statistical package for social science (SPSS). The results obtained showed a mathematical model predicting bead geometry for any circumstance. These results indicate that the welding current and arc voltage are the ones that significantly affect the bead width. Dutta and Dilip in (2007) [7], determined input and output relationships in TIG welding process. The study aims to compare between Adaptive Neuro-Fuzzy interface system model and Regression model. Two neural network-based approaches (back propagation algorithm and genetic neural system) and conventional regression based on full factorial design of experimental (DOE). The input parameters of the process are speed of welding, rate of wire feed %, gap rate, welding current, while the output parameters are front and back height, front and back width of TIG welding process. Karabulut et al. in (2016) [8] used SAW welding of steel under different welding parameters. They compare the microstructure before and after welding. The microstructure test shows that ferrite and pearlite) is the structure before welding, while the structure of welded samples contains ferrite only. Widmanstatten, also, near the HAZ polygonal and plate ferrite in weld material. Increasing welding current lead to heat input increases, thus HAZ will also increase. The increasing in welding current encourages the formation of Widmanstatten ferrite. The hardness is increased when the welding current is increased due to high austenite formation at large cooling rate. Habibi et al. in (2018) [9], investigated the formability of mechanical properties and (FLDs) of (TWBs) produced by (FSW) process. The difference of thicknesses and directions were compared with base metals and with each other. When the welded material is all kinds of steel with yield strength less than 180 MPa or mild steel were used in friction stir welding (FSW) process the appropriate of material is tungsten carbide. Suitable rotational speeds and feed for carrying out the FSW process were 1100 rpm and 60 (mm per min) respectively. It has been found in this type of welding to the hardness increase as we approached the center of weld. The welded zone has three region different properties. Also, welded zone center was finer grains size. Using the Nakazima method to investigate the tailored blanks FLDs, it is clear to find out that there is formability decreasing in the difference of thickness and welding process.

2. Experimental Part

In this work, Low Carbon steel plates (AISI 1020) 16 mm (5/8 in) thick is used as a base metal for the experimental work. It is widely used in steel structure, i.e. (pressure tanks, building structures, vessels and pipeline for petroleum industries). These plates are cut to dimensions of (125 × 250 × 16 mm). Both surfaces are cleaned to remove oxides, dirt and rust before welding. The chemical composition of the carbon steel is shown in the Table 1.

Twenty seven pairs of carbon steel plates have been prepared before the weld and machined to the required dimensions (250 × 250 × 16 mm). V-groove partial penetration-butt joint with 8 mm face root and angle of 60° with 2 mm opening (gap between two specimens) was prepared to fabricate SAW joints as shown Fig. 1. The preparation of all specimens joint edges (bevels) was done by grinding machine, (disc polishing).

Table 1 Chemical composition of AISI 1020 carbon steel.

Element	ASTM (%)	Test (%)
C	0.26	0.19-0.21
Fe	99.00	98.6-98.7
Mn	0.75	0.53-0.54
P	≤0.04	0.050
S	≤0.05	0.030-0.043

Table 2 Mechanical properties of AISI 1020 carbon steel.

Ultimate tensile stress (MPa) Min.		Yield stress (MPa) Min.		Impact (J) Min.	
Standard	Test	Standard	Test	Standard	Test
380	405	205	261	126	112

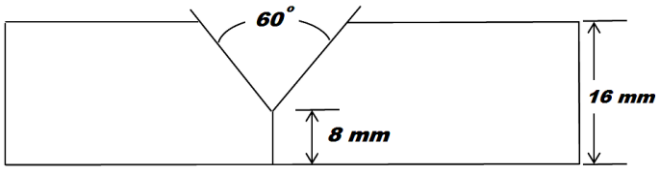

Fig. 1 V-groove partial penetration- butt joint.

SAW Machine type lincoln electric machine type was used in this work. The advantages of SAW machine is that the machine working on both automatic and manual modes. The input parameters of the machine and orthogonal array are shown in Appendix A. The specimens are linked by single pass arc welding with AWS electrode type E6010 with diameter equal to 3.25 mm before using SAW welding machine. The SAW welding machine use a 3.2 mm diameter wire type EN ISO 544: B 300 and the flux used according to AWS A5.17/A5.23: F6 A4-EL and DIN EN 760: SA MS 188 AL H5, has been used as the welding consumable electrode.

2.1. Tensile Test

Tensile test is one of the most common destructive tests. The sample was prepared according to ASME IX-2017 (QW-151.2) and API-STANDARD-1104 (5.6.3) and the samples were made as a vertical piece on the welding direction as shown in Fig. 2. The tensile sample is broken from either the weld area if it contains defects or from the base metal in HAZ.

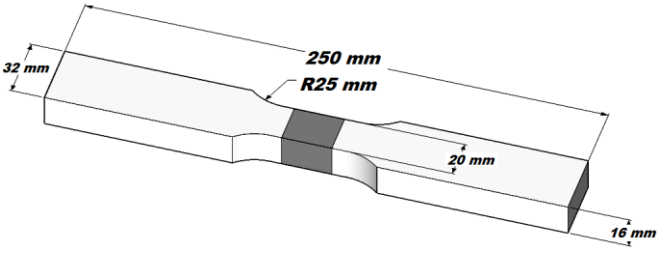

Fig. 2 Dimensions of tensile testing specimen.

2.2. Impact Test

The test is a measure the absorbed energy of material. Absorbed energy measured from the sample depending on the amount of energy absorbed from the broken sample and the sample is perpendicular on the direction of the weld. The

sample contains a chisel (V) at 45 angle, 2 mm depth, dimensions according to ASME (QW-463.1(f)), as shown in Fig. 3 and 4 after the test.

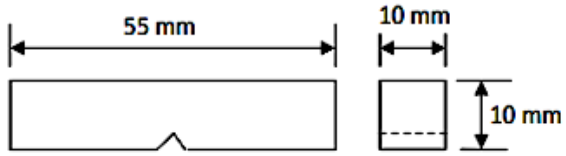

Fig. 3 Dimensions of impact testing specimen.

Fig. 4 Impact specimen after test.

2.3. Micro Hardness Test

To test the hardness, the sample should be divided into several regions (weld metal, HAZ and base metal), the specimens shows in Fig. 5 and 6.

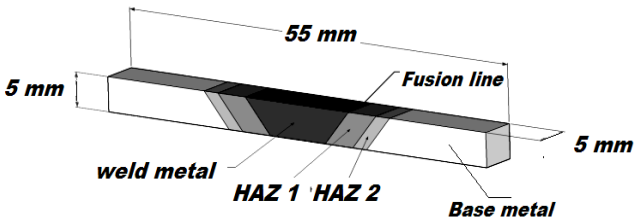

Fig. 5 Regions of the specimen after weld.

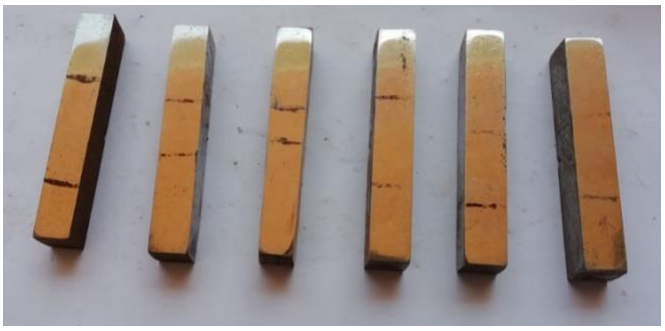

Fig. 6 Specimens after polish for micro hardness test.

3. Results and Discussion

3.1. Neuro-Fuzzy

Experimental process needs much time and cost. Table 4 show experimental results. This experimental data was involved in the ANFIS model Table 5 to 8. Several experiments were conducted for a certain number of membership functions that including (Gaussian, Gaussian 2, Triangular, Trapezoidal, Generalized bell, Π), as shown in Tables 5 to 8. Also used generalized bell membership functions with three number of membership functions give the best performance for ultimate tensile stress predicted, and generalized bell membership functions with three number of membership functions give the best performance for yield stress predicted, and Triangular membership functions with two number of membership functions give the best performance for predicting impact energy, generalized bell membership functions with three number of membership functions give the best performance for ultimate tensile stress predicted as show in Table 9.

Table 4 Results of experimental tests.

No. SP.	Current (A)	Voltage (V)	WS (cm/min)	UTS (MPa)	Yield stress (MPa)	Impact (J)	Hardness at center weld (Hv)
1	380	25	25	435	308	200	228
2	380	25	30	442	313	206	235
3	380	25	40	446	318	213	241
4	380	30	25	434	301	155	229
5	380	30	30	436	308	200	237
6	380	30	40	441	317	204	244
7	380	35	25	432	300	152	232
8	380	35	30	434	303	163	240
9	380	35	40	440	309	176	245
10	420	25	25	429	302	162	233
11	420	25	30	440	307	166	239
12	420	25	40	444	312	175	243
13	420	30	25	435	297	141	236
14	420	30	30	437	300	153	239
15	420	30	40	439	314	167	246
16	420	35	25	432	299	155	240
17	420	35	30	435	303	151	245
18	420	35	40	436	308	168	248
19	460	25	25	439	298	155	238
20	460	25	30	430	301	158	243
21	460	25	40	434	304	169	244
22	460	30	25	424	296	138	246
23	460	30	30	428	299	149	248
24	460	30	40	435	300	152	249
25	460	35	25	431	296	150	247
26	460	35	30	433	299	158	255
27	460	35	40	435	304	168	259

Table 5 Performance of ANFIS model for different membership functions to predict the ultimate tensile stress.

Type of MFs	NO. of MFs	Training		Testing	
		R	MSE	R	MSE
Gaussian	3	1	1.3690e-11	0.80168	8.8768
Gaussian2	4	1	7.1235e-12	0.79123	6.9999
Triangular	3	1	3.2552e-12	0.79123	13.8306
Trapezoidal	2	0.99973	0.0145	0.4089	992.36213
Generalized bell	3	1	1.2594e-11	0.79995	6.4615
Π	2	0.99974	0.0136	0.34194	3161.8357

Table 6 Performance of ANFIS model for different membership functions to predict the yield stress.

Type of MFs	NO. of MFs	Training		Testing	
		R	MSE	R	MSE
Gaussian	4	1	1.2496e-10	0.80696	51.5799
Gaussian2	4	1	1.4739e-11	0.41541	53.6714
Triangular	4	1	1.4672e-11	0.41541	54.0397
Trapezoidal	3	1	1.5663e-11	0.14558	66.9908
Generalized bell	**3**	**1**	**3.0617e-11**	**0.68386**	**32.2016**
Π	2	1	7.3300e-06	0.3777	873.1626

Table 7 Performance of ANFIS model for different membership functions to predict the impact energy.

Type of MFs	NO. of MFs	Training		Testing	
		R	MSE	R	MSE
Gaussian	2	0.99939	0.5392	0.65508	182.7996
Gaussian2	2	0.99952	0.4242	0.52199	235.8500
Triangular	**2**	**0.99932**	**0.5962**	**0.751**	**156.4026**
Trapezoidal	2	0.99952	0.4197	0.51439	238.5297
Generalized bell	3	1	1.1236e-10	0.62288	235.9844
Π	2	0.99957	0.3758	0.43771	266.9183

Table 8 Performance of ANFIS model for different membership functions to predict the hardness.

Type of MFs	NO. of MFs	Training		Testing	
		R	MSE	R	MSE
Gaussian	5	0.99166	0.9864	0.95209	7.4852
Gaussian2	4	1	1.2969e-11	0.82016	6.9288
Triangular	2	0.99993	0.0084	0.82185	0.8218
Trapezoidal	3	1	6.8967e-12	0.86307	15.0128
Generalized bell	3	1	1.3400e-11	0.99532	4.7059
Π	3	1	6.6434e-12	0.87754	18.2218

Table 9 The best performance for predicting the mechanical properties.

Output parameter	Type of MFs	NO. of MFs	Training		Testing	
			R	MSE	R	MSE
UTS	Generalized bell	3	1	1.2594e-11	0.7999	6.4615
Yield stress	Generalized bell	3	1	3.0617e-11	0.6839	32.2016
Impact energy	Triangular	2	0.9993	0.5962	0.751	156.403
Hardness	Generalized bell	3	1	1.3400e-11	0.9953	4.7059

3.2. Direct Effect of Saw Parameters on Properties of Welded Plates and Geometry

3.2.1. Effect Welding Current on Plate's Welded and Geometry

As the current increased from 380 to 460 A, the ultimate tensile stress decreased and the yield stress decreased as shown in Fig. 7. When the current is increased welding heat input increases, which means that (the heat input is directly proportional to the current value). Therefore any reduction in the UTS and yield stress is because of the increase of heat input and temperature [10].

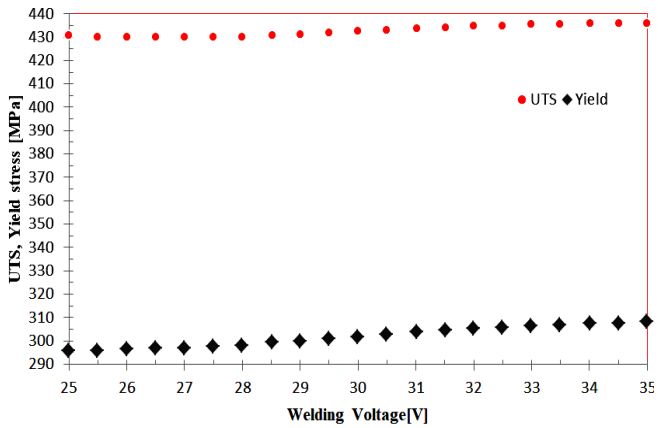

Fig. 7 Effect of current on the tensile strength and yield strength.

From Fig. 8, it can be observed that the current increase from (380 to 460) A, the impact energy decreases. This decrease is because heat input is directly proportional to the current value, which means increase the temperature with welding current [11].

Effect the welding variable on the hardness of the joints welded, Fig. 8 shows that the hardness of the welded sample increased when the increase welding current from (380 to 460) A, because it is possible that more Widmanstatten ferrite or martensite structure can be formed [8].

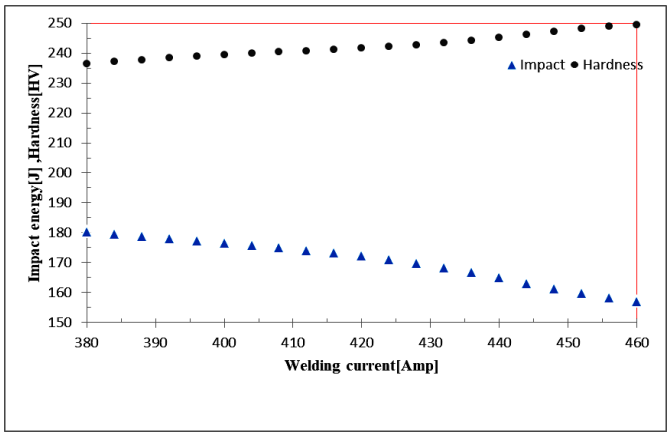

Fig. 8 Effect of current on the impact energy and hardness.

3.2.2. Effect Arc Voltage on Plate's Welded and Geometry

The effect of voltage on ultimate tensile stress and yield strength for the welded are shown in Fig. 9. However increase in welding voltage from 25 to 35 V will increase the ultimate tensile stress and the yield stress [10]. This increase is because of the heat input inversely proportional to voltage [12]. Then the ultimate tensile stress and yield stress increase with welding voltage increase.

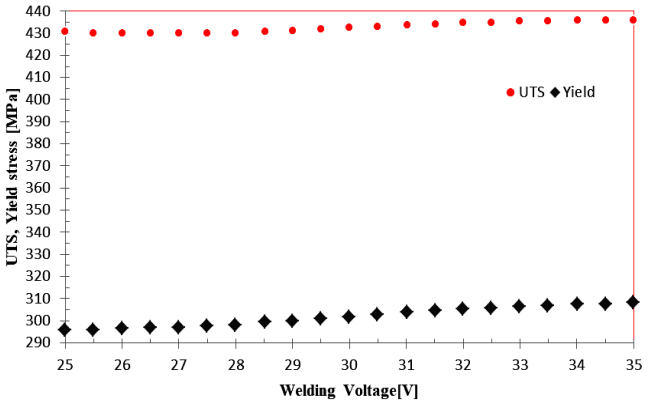

Fig. 9 Effect of voltage on the UTS and yield stress.

The effect of arc voltage is shown in Fig. 10, where increasing arc voltage (from 25 to 35) V, the impact energy increases, this increase because the heat input inversely proportional to voltage welded.

The hardness increase with increasing the arc voltage (from 25 to 35) V [11], as shown the Fig. 10.

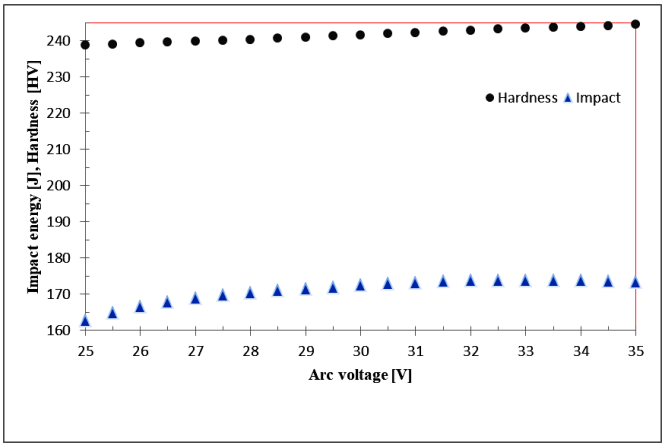

Fig. 10 Effect of voltage on the impact energy and Hardness.

3.2.3. Effect Welding Speed on Plate's Welded and Geometry

Increase in welding speed from (25 to 40) cm/min decreases the ultimate tensile stress and yield stress respectively. The range of welding speed increase the UTS and yield stress will decrease as shown in Fig. 11.

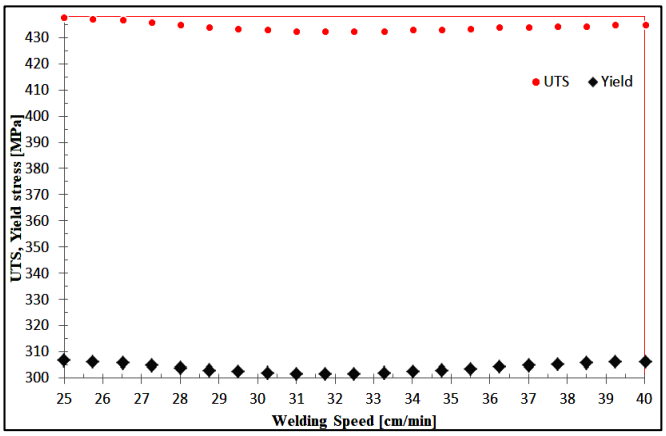

Fig. 11 Effect of welding speed on the UTS and yield stress.

An increasing welding speed (from 25 to 40) cm/min the impact energy decrease as shown the Fig. 12, when the welding speed increasing we can't obtain on the heat input enough because this effected during the range is limited [11].

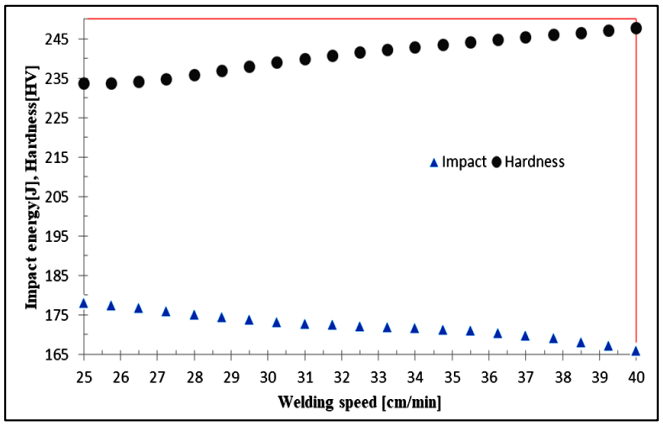

Fig. 12 Effect of welding speed on the impact energy and hardness.

The hardness increase with increasing of the welding speed from 25 to 40 cm/min, as shown in Fig. 12. The increased in hardness due to increase deposition and the deposition is directly proportional to the current, voltage and welding speed [11].

3.3. Regression Model

Regression procedure is used to develop the required mathematical model for estimate the ultimate tensile stress, yield stress, impact energy, and hardness. The response function representing the strength of welded plates by Y = f (WC, AV, WS). Equation (1) shows the 2nd order polynomial (surface factor k) [10].

$$Y = b_o + \sum_{i=1}^{k} b_i x_i + \sum_{i=1}^{k} b_{ii} x_{ii}^2 + \sum_{i<j} b_{ij} x_i x_j \quad (1)$$

Where, b_o is the free term of the regression equation. b_1, b_2, b_3 and b_4 are coefficients linear terms. b_{11}, b_{22}, b_{33}, b_{44} and b_{55} are quadratic terms the coefficients. b_{12}, b_{13}, b_{14}, b_{15}, b_{55}, b_{23}, b_{24}, b_{25}, b_{34}, b_{35} and b_{45} are coefficients interaction terms. k is number of trails.

IBM SPSS Statistical 24 was used to calculate the values of these coefficients. The mathematical models that calculate by the above analysis are represented below:

$$\text{Ultimate tensile stress} = (-0.274 * WC - 0.109 * AV + 0.339 * WS - 0.135 * WC^2 - 0.182 * WS^2 + 0.189 * WC * AV - 0.065 * WC * WS - 0.117 * AV * WS) * 11 + 438.157 \quad (2)$$

$$\text{Yield stress} = (-0.577 * WC - 0.182 * AV + 0.551 * WS - 0.226 * WC^2 + 0.104 * AV^2 - 0.057 * WS^2 + 0.223 * WC * AV - 0.026 * WC * WS - 0.022 * AV * WS) * 11 + 305.02 \quad (3)$$

$$\text{Impact energy} = (-0.366 * WC - 0.211 * AV + 0.25 * WS - 0.331 * WC^2 - 0.152 * AV^2 - 0.14 * WS^2 + 0.315 * WC * AV - 0.114 * WC * WS - 0.008 * AV * WS) * 37.5 + 160.688 \quad (4)$$

$$\text{Hardness} = (0.36 * WC + 0.252 * AV + 0.306 * WS + 0.102 * WC^2 + 0.055 * AV^2 - 0.169 * WS^2 + 0.14 * WC * AV - 0.129 * WC * WS - 0.006 * AV * WS) * 15.5 + 242.803 \quad (5)$$

Tables 9 to 12 show the predicted ANFIS and regressions analysis results by using six test data sets. The maximum error between experimental and ANFIS is 0.9195 %, the mean error rate is 0.5352 % and the correlation coefficient 0.7912. While, maximum error between experimental and regression analysis results is 2.937 %, the mean error rate is 0.92 % and the correlation coefficient squared 0.864. The maximum error between experimental and ANFIS is 3.3713, the mean error rate is 1.4148 % and the correlation coefficient 0.6839. While, maximum error between experimental and regression analysis results is 2.878 %, the mean error rate is 1.9863 % and the correlation coefficient squared 0.923. The maximum error between experimental and ANFIS is 17.7472 %, the mean error rate is 5.3535 % and the correlation coefficient 0.65508. While, maximum error between experimental and regression analysis results is 7.398 %, the mean error rate is 0.3587 % and the correlation coefficient squared 0.876. The maximum error between experimental and ANFIS is 1.4665 %, the mean error rate is 0.8165 % and the correlation coefficient 0.99532. While, maximum error between experimental and regression analysis results is 1.764 %, the mean error rate is 0.6238 % and the correlation coefficient squared 0.979. The maximum error between experimental and ANFIS is 7.9223 %, the

mean error rate is 3.1838 % and the correlation coefficient 0.80367. While, maximum error between experimental and regression analysis results is 19.203 %, the mean error rate is 11.4588 % and the correlation coefficient squared 0.886. The maximum error between experimental and ANFIS is 34.945 %, the mean error rate is 19.2069 % and the correlation coefficient 0.98061. Moreover, maximum error between experimental and regression analysis results is 133.1 %, the mean error rate is 79.3885 % and the correlation coefficient squared 0.517.

- Percentage of error = $\left|$(actual value – predicate value)/ predicate value$\right|$ * 100 %
- Mean error = $\sum$ percentage of error$/\epsilon$

Table 9 Comparison between the experimental and the predicted ANFIS model results of welded plate's strength.

Ultimate tensile stress (MPa)			Yield stress (MPa)		
EXP	**ANFIS model**	**Error %**	**EXP**	**ANFIS model**	**Error %**
431	435	0.9195	298	296.881	0.3770
433	435	0.4598	300	299.794	0.0688
434	435	0.2299	301	302.226	0.4056
436	437	0.2288	304	299.033	1.6611
440	436	0.9174	309	301.155	2.6048
441	439	0.4556	313	302.792	3.3713
Mean error %		0.5352	Mean error %		1.4148
Correction coefficient		0.79123	Correction coefficient		0.68386

Table 10 Comparison between the experimental and the predicted ANFIS model results of welded plates of the impact energy and hardness.

Impact energy (J)			Hardness (Hv)		
EXP.	**ANFIS model**	**Error %**	**EXP**	**ANFIS model**	**Error %**
151	162.302	6.9637	237	239.602	1.0858
153	151.942	0.6963	240	240.881	0.3656
155	148.239	4.5608	239	240.486	0.6178
167	167.18	0.1079	245	243.266	0.7128
176	179.674	2.0449	246	244.411	0.6502
200	169.855	17.7472	249	245.401	1.4665
Mean error %		5.3535	Mean error %		0.8165
Correction coefficient		0.65508	Correction coefficient		0.99532

Table 11 Comparison between the experimental and the predicted regression model results of welded plate's strength.

Ultimate tensile stress (MPa)			Yield stress (MPa)		
EXP	regression model	Error %	EXP	regression model	Error %
428	432.4309	1.025	299	294.002	1.700
433	433.7399	0.171	299	295.6773	1.124
424	428.642	1.083	296	289.213	2.347
430	431.1219	0.260	301	294.614	2.168
439	426.475	2.937	298	289.664	2.878
431	430.809	0.044	296	291.05	1.701
Mean error %		0.9200	Mean error %		1.9863
Correction coefficient squared		0.864	Correction coefficient squared		0.923

Table 12 Comparison between the experimental and the predicted regression model results of welded plates of the impact energy and hardness.

Impact energy (J)			Hardness (kJ)		
EXP.	**regression model**	**Error %**	**EXP**	**regression model**	**Error %**
149	157.0917	5.151	248	248.7579	0.305
158	166.5917	5.157	255	255.6554	0.256
138	149.025	7.398	246	244.6005	0.572
158	158.9917	0.624	243	243.5654	0.232
155	151.125	2.564	238	239.47	0.614
150	158.325	5.258	247	251.436	1.764
Mean error %		0.3587	Mean error %		0.6238
Correction coefficient squared		0.876	Correction coefficient squared		0.979

4. Conclusion

In this work welded plates were used for AISI1020 material by using ANFIS and regression analysis. Thus, they are used multi-input-single-output included (ultimate tensile stress, yield stress, impact energy, hardness) and used for Adaptive Neuro-Fuzzy Interface System and regression analysis. The most important conclusions that can be drawn from this study can be summarized as follows:

1. The compared ANFIS with experimental results the correlation coefficient and mean error are 0.79123, 0.5352 %, 0.68386, 1.4148 %, 0.65508, 5.3535 %, 0.99532, 0.8165 %, 0.80367, 3.1838 %, 0.98061, 19.2069 % respectively.
2. The regression analysis compared with experimental results the correlation coefficient and mean error are 0.864, 0.92 %, 0.923, 1.9863 %, 0.876, 0.3587 %, 0.979, 0.6238 %, 0.886, 11.4588 %, 0.517, 79.3885 % respectively. From above value conclude that prediction ANFIS better than regression.
3. The effect of input parameter on the output parameter:
   a) The ultimate tensile stress increases with increasing arc voltage, while ultimate tensile stress decreases with increasing welding current and welding speed.
   b) The yield stress increases with increasing arc voltage, while yield stress decrease with increasing welding current and welding speed.
   c) The impact energy increases with increasing arc voltage, while impact energy decrease with increasing welding current and welding speed.
   d) The hardness increases with increasing welding current arc voltage and welding speed.

Appendices

Input parameters and their levels of SAW process.

Input process parameters	Notation	Unit	Max. value +1	Medium Value 0	Min. value -1
Welding speed	WS	cm/min	40	30	25
Arc voltage	AV	V	35	30	25
Welding Current	WC	A	460	420	380

Orthogonal array of input parameters.

Sample No.	Current (A)	Voltage (V)	Welding speed (cm/min)
1	-1	-1	-1
2	-1	-1	0
3	-1	-1	+1
4	-1	0	-1
5	-1	0	0
6	-1	0	+1
7	-1	+1	-1
8	-1	+1	0
9	-1	+1	+1
10	0	-1	-1
11	0	-1	0
12	0	-1	+1
13	0	0	-1
14	0	0	0
15	0	0	+1
16	0	+1	-1
17	0	+1	0
18	0	+1	+1
19	+1	-1	-1
20	+1	-1	0
21	+1	-1	+1
22	+1	0	-1
23	+1	0	0
24	+1	0	+1
25	+1	+1	-1
26	+1	+1	0
27	+1	+1	+1

References

[1] George E. Linnert, Welding Metallurgy Carbon and Alloy Steels, Fourth edition, Hilton Head Island, USA, 2002.

[2] J. I. Lee, K. W. Um, "A prediction of welding parameters by prediction of back-bead geometry", Elsevier, Journal of Materials processing technology, Vol. 108, Issue 1, pp. 106-113, 2000.

[3] S. C. Juang, Y. S. Tarng, "Process parameter for optimizing the weld pool geometry in the tungsten inert gas welding of stainless steel", Elsevier, Journal of Materials processing technology, Vol. 122, Issue 1, pp. 33-37, 2002.

[4] Qian Hancheng, Xia Bocaib, Li Shangzheng, Wang Fagen, "Fuzzy neural network modeling of material properties", Elsevier, Journal of Materials Processing Technology, Vol. 122, pp. 196-200, 2002.

[5] I. S. Kim, J. S. Son, I. G. Kim, J. Y. Kim and O. S. Kim, "A study on relationship between process variables and bead penetration for robotic CO_2 arc welding", Elsevier, Journal of Materials Processing Technology, Vol. 136, pp. 139-145, 2003.

[6] S. Kumanan, J. Edwin Raja Dhas K. Gowthaman, "Determination of submerged arc welding process parameter using Taguchi method and regression analysis", Indian Journal engineering & Materials Sciences, Vol. 14, pp. 177-183, 2007.

[7] Parikshit Dutta, Dilip Kumar Pratihar, "Modeling of TIG welding process using conventional regression analysis and neural- based approaches", Elsevier, Journal of Materials Processing Technology, Vol. 184, pp. 56-68, 2007.

[8] Hasan Karabulut, Mustafa Türkmen, Mehmet Akif Erden and Süleyman Gündüz, "Effect of Different Current Values on Microstructure and Mechanical Properties of Microalloyed Steels Joined by the Submerged Arc Welding Method", Article Metals, 2016.

[9] M. Habibi, R. Hashemi, M. Fallah Tafti, A. Assempour, "Experimental investigation of mechanical properties, formability and forming limit diagrams for tailor-welded blanks produced by friction stir welding", Journal of Manufacturing Processes, Vol. 31, pp. 310-323, 2018.

[10] Falah Mustafa Al-Saraireh, "The effect of current and voltage on mechanical properties of low carbon steel products", Faculty of Engineering Mutah University, Al-Karak, Jordan, Vol. 9, pp. 134-142, 2018.

[11] S. I. Talabi, O. B. Owolabi, J. A. Adebisi, T. Yahaya, "Effect of welding variables on mechanical properties of low carbon steel welded joint", Journal Advance in Production Engineering & Management, Vol. 9, pp. 181-186, 2014.

[12] Raad Jamal Jassim, "Parametric Study of Gas Metal Arc Welding for ASTM A283 Steel Weldments Using Experimental, Neural and Genetic Procedures", Ph.D. Thesis, University of Basrah, 2013.